Supporting information

Fluid Guided CVD Growth for Large-scale Monolayer Two-dimensional Materials

Dong Zhou [a,b,#], Ji Lang[a,c,#], Nicholas Yoo[b,d], Raymond R. Unocic[e], Qianhong Wu[a,c,*], Bo Li[a,b,*]

[a]Department of Mechanical Engineering, Villanova University, Villanova, PA, 19085, United States

[b]Hybrid Nano-Architectures and Advanced Manufacturing Laboratory, Villanova University, Villanova, PA, 19085, United States

[c]Cellular Biomechanics and Sports Science Laboratory, Villanova University, Villanova, PA, 19085, United States

[d]Department of Chemical and Biological Engineering, Villanova University, Villanova, PA, 19085, United States

[e]Center for Nanophase Materials Sciences, Oak Ridge National Laboratory, Oak Ridge, Tennessee, 37831, United Statess

E-mail: qianhong.wu@villanova.edu (Q.W.); bo.li@villanova.edu (B. L.)

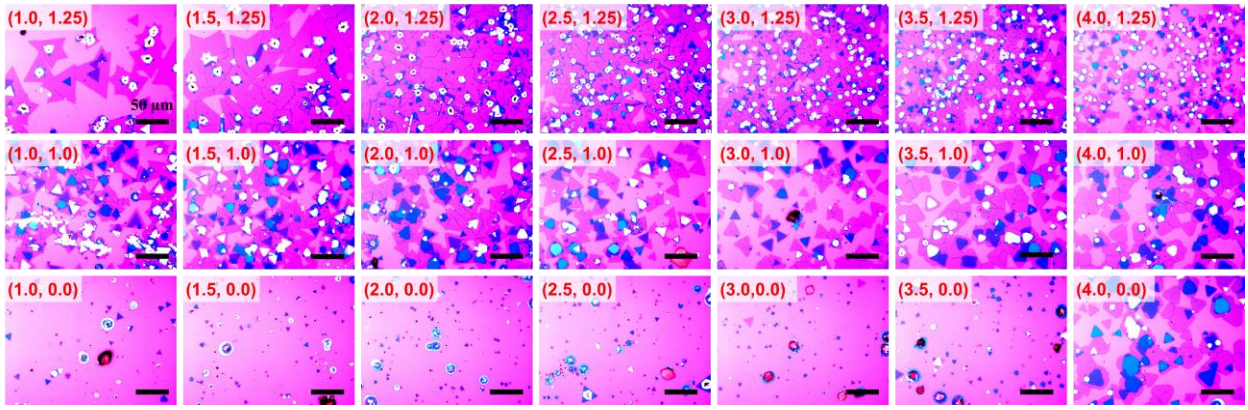

Figure S1. The detailed morphology distribution over the substrate using the standard APCVD.

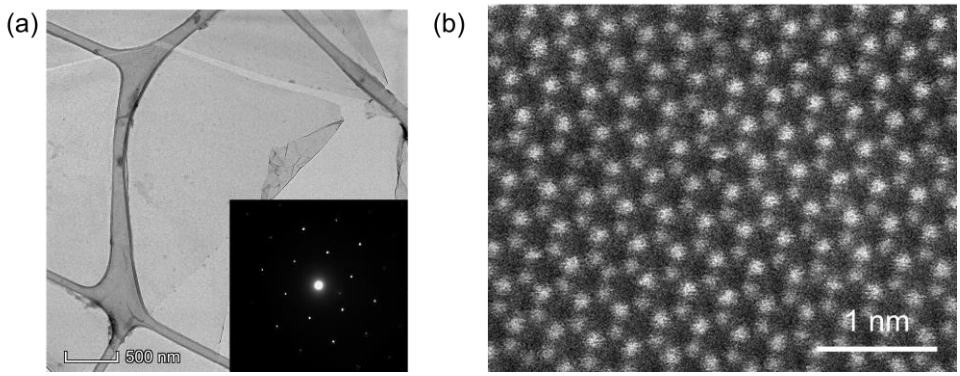

Figure S2. (a) TEM image of monolayer $MoSe_2$ with inset selected area electron diffraction pattern and (b) annular dark field STEM image of monolayer $MoSe_2$.

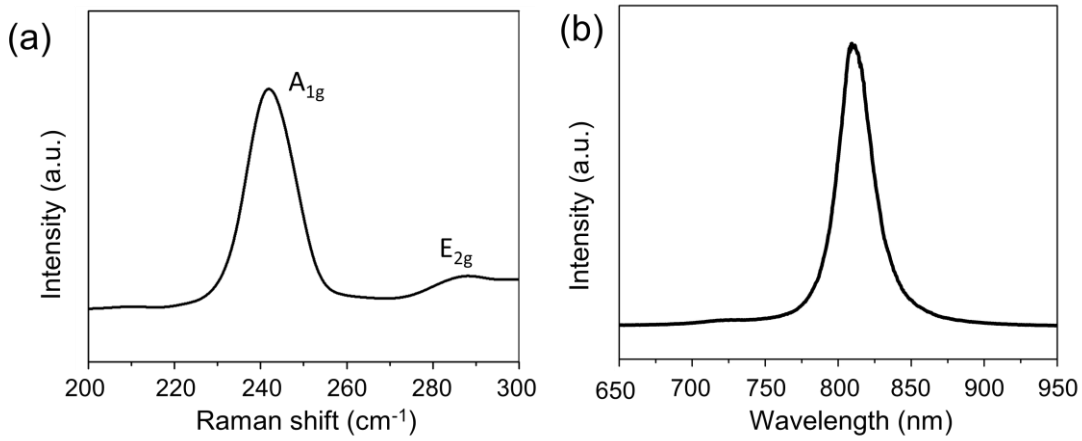

Figure S3. The Raman (a) and PL(b) spectra of the monolayer $MoSe_2$.

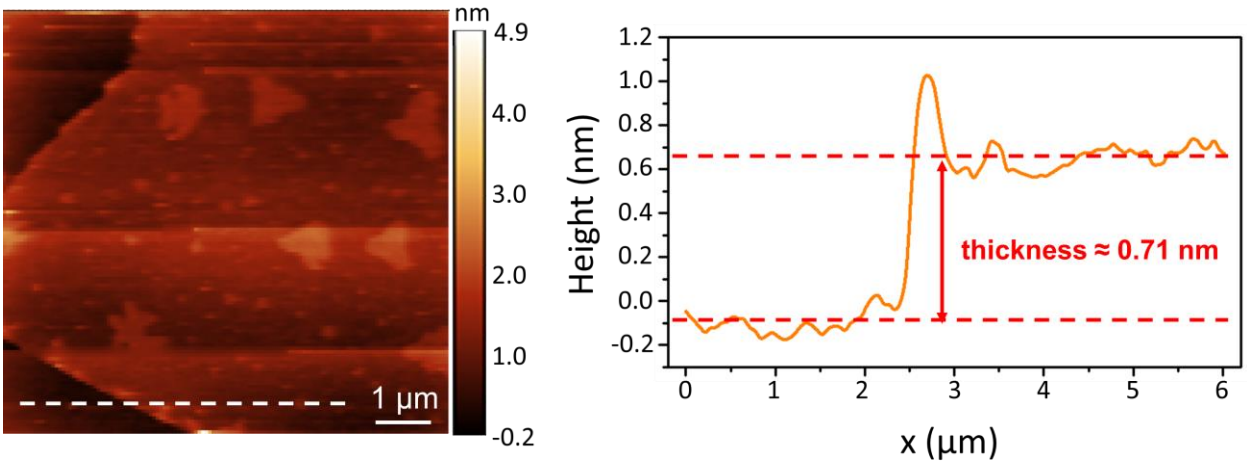

Figure S4. Atomic force microscope (AFM) topography of the monolayer $MoSe_2$ flakes.

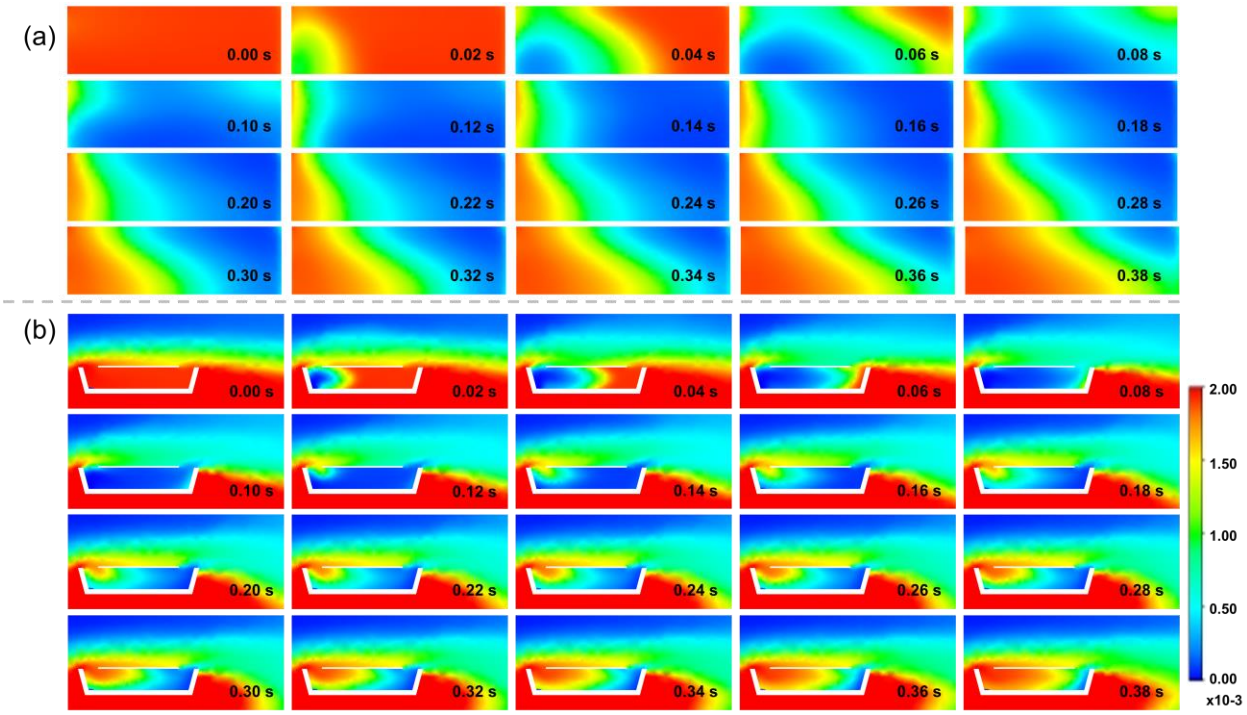

Figure S5. Se concentration evolution in the standard APCVD growth process. (a) top view, (b) cross-sectional view.

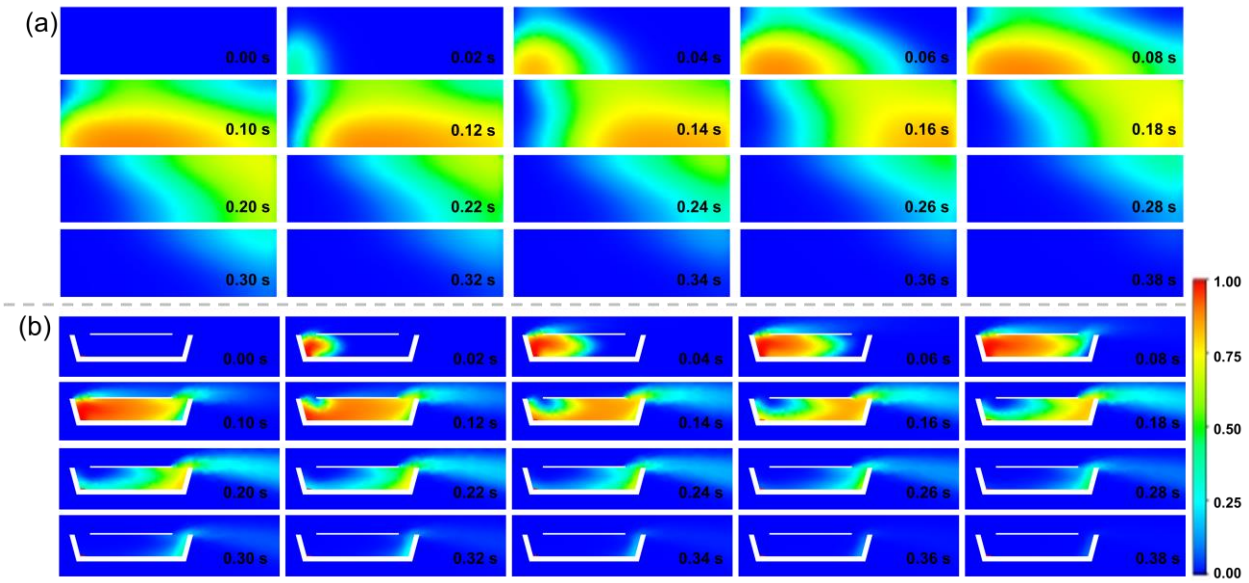

Figure S6. MoO_3 concentration evolution in the standard APCVD growth process. (a) top view, (b) cross-sectional view.

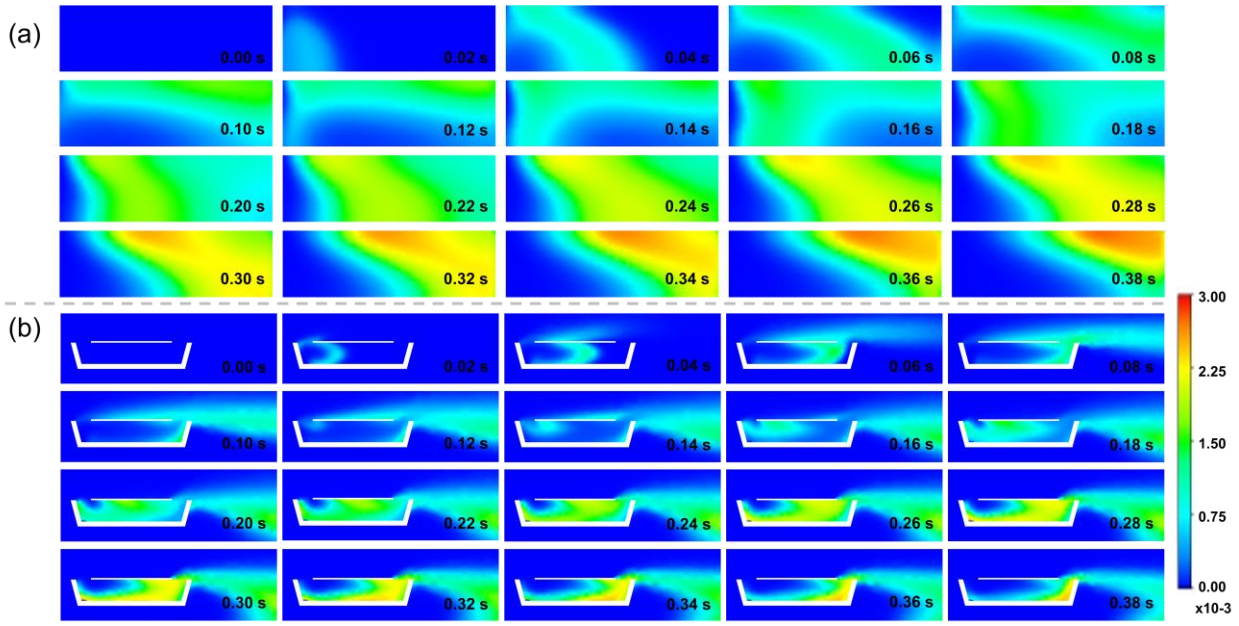

Figure S7. $MoSe_2$ concentration evolution in the standard APCVD growth process. (a) top view, (b) cross-sectional view.

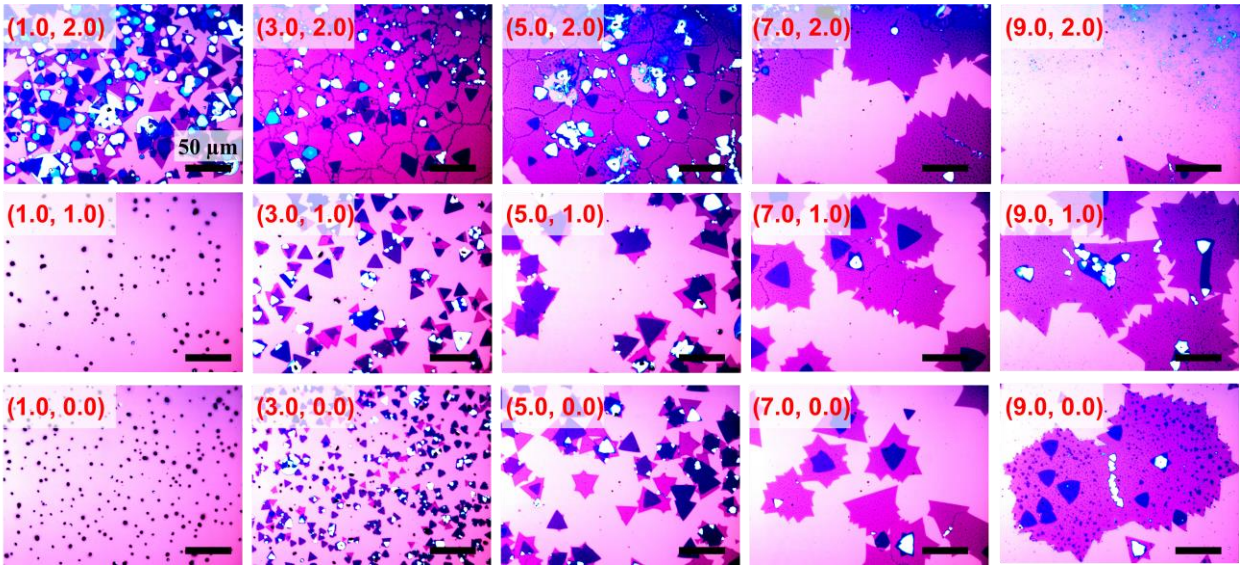

Figure S8. The detailed morphology distribution over the substrate using the flipped APCVD.

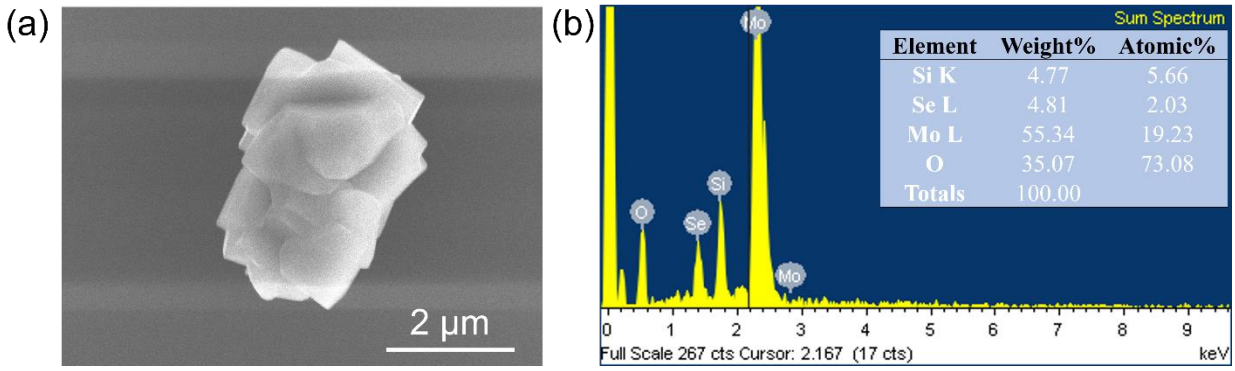

Figure S9. (a) The SEM image of deposited particles. (b) The Energy-dispersive X-ray spectroscopy (EDX) analysis of (a).

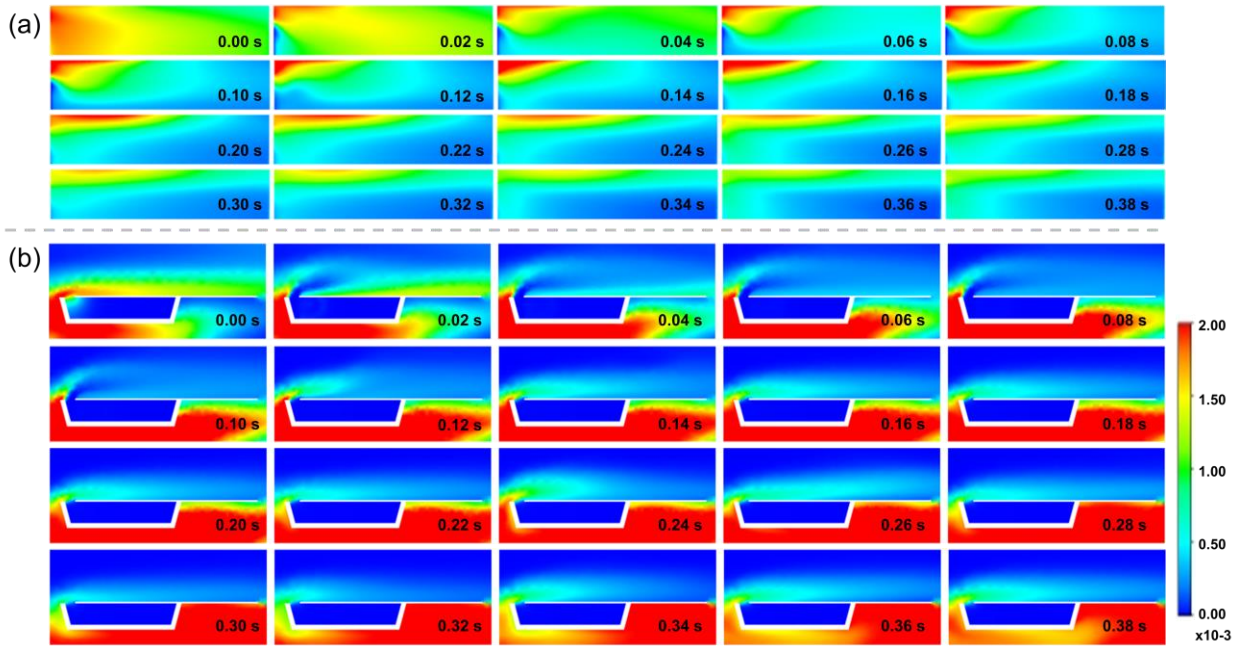

Figure S10. Se concentration evolution in the flipped APCVD growth process. (a) top view, (b) cross-sectional view.

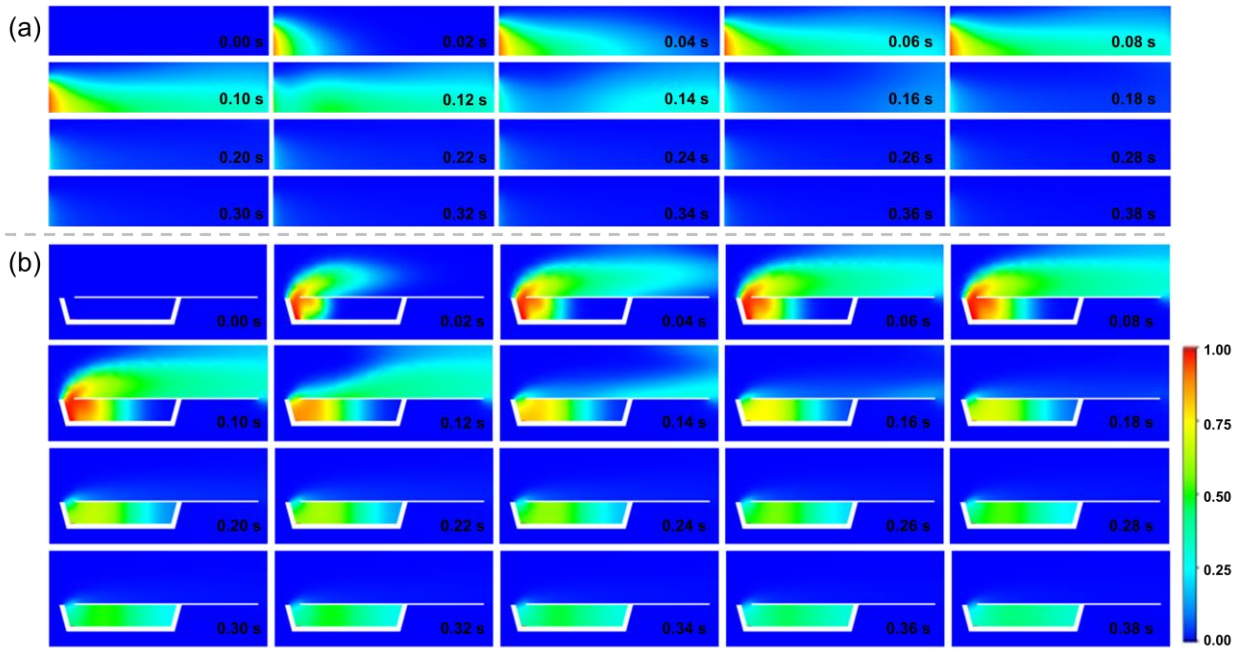

Figure S11. MoO_3 concentration evolution in the flipped APCVD growth process. (a) top view, (b) cross-sectional view.

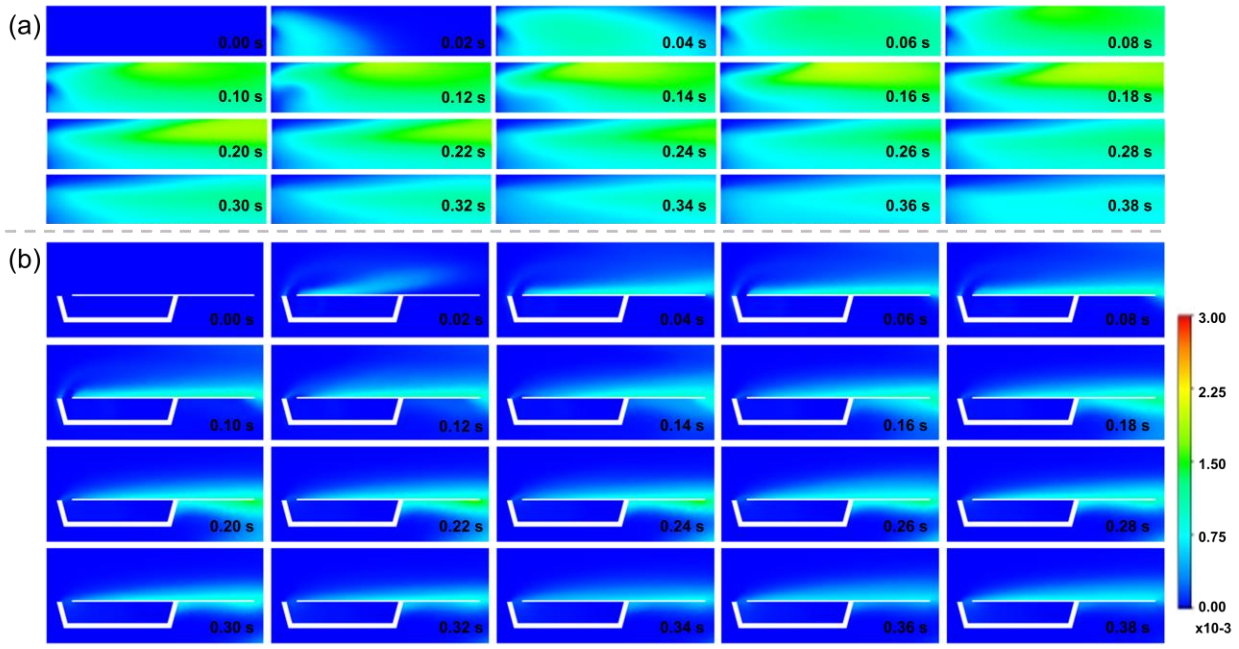

Figure S12. $MoSe_2$ concentration evolution in the flipped APCVD growth process. (a) top view, (b) cross-sectional view.

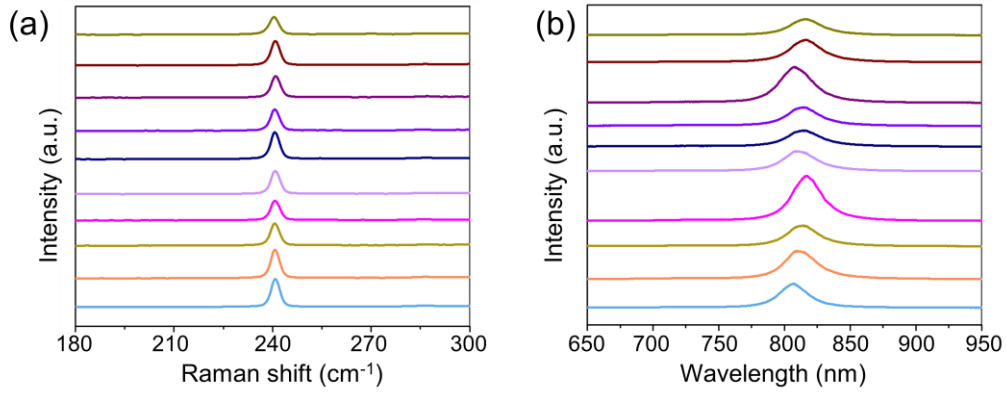

Figure S13. 10 Random Raman and PL spectra of $MoSe_2$ film obtained by the evolved setup.

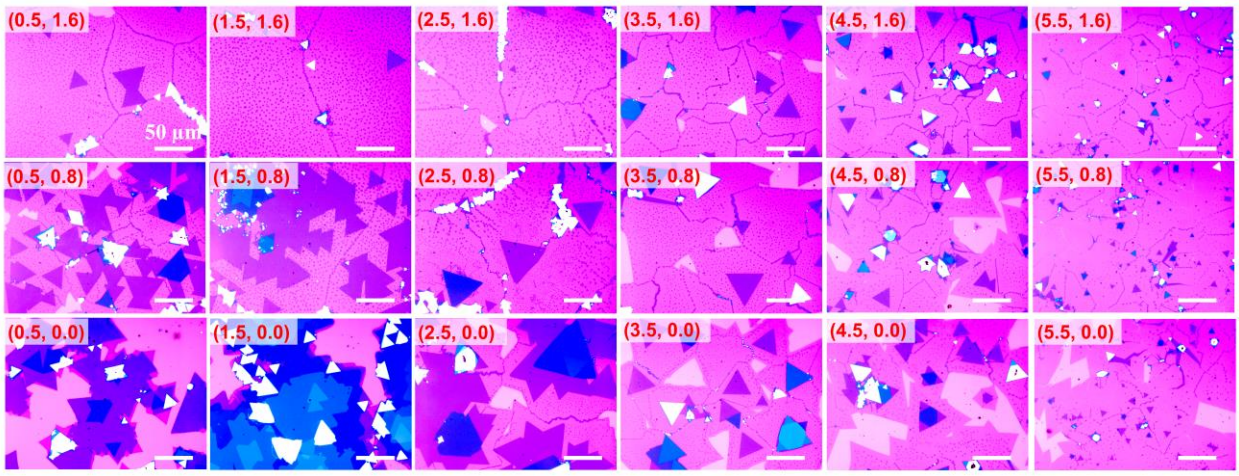

Figure S14. The detailed morphology distribution over the substrate using the evolved APCVD.

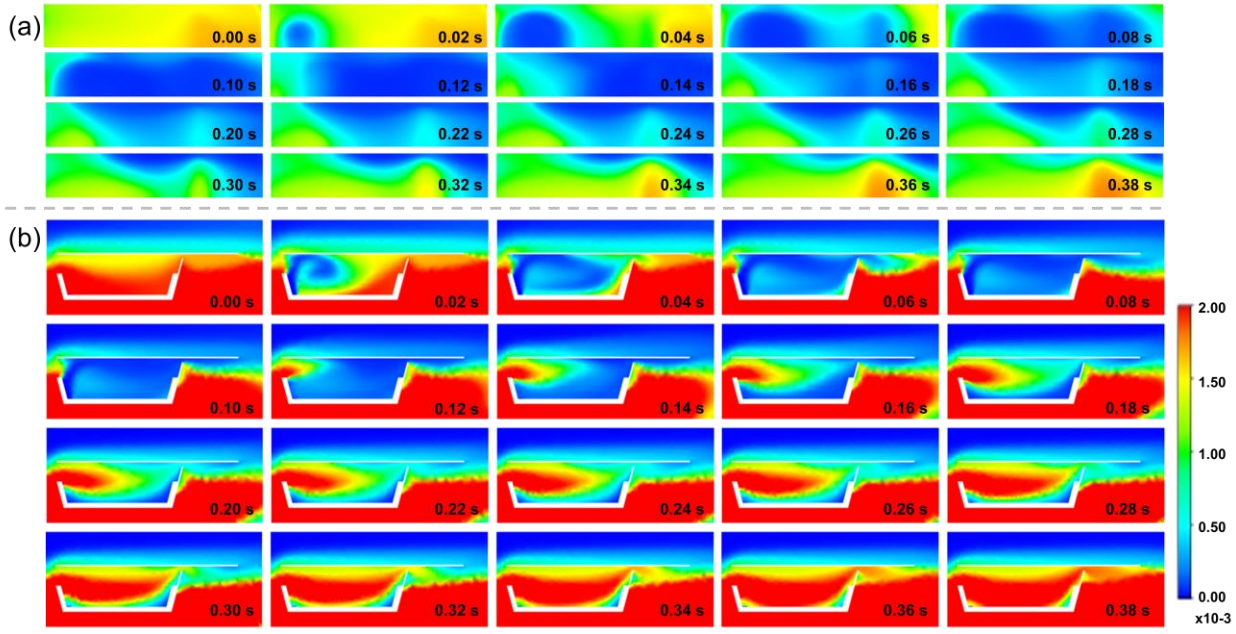

Figure S15. Se concentration evolution in the evolved APCVD growth process. (a) top view, (b) cross-sectional view.

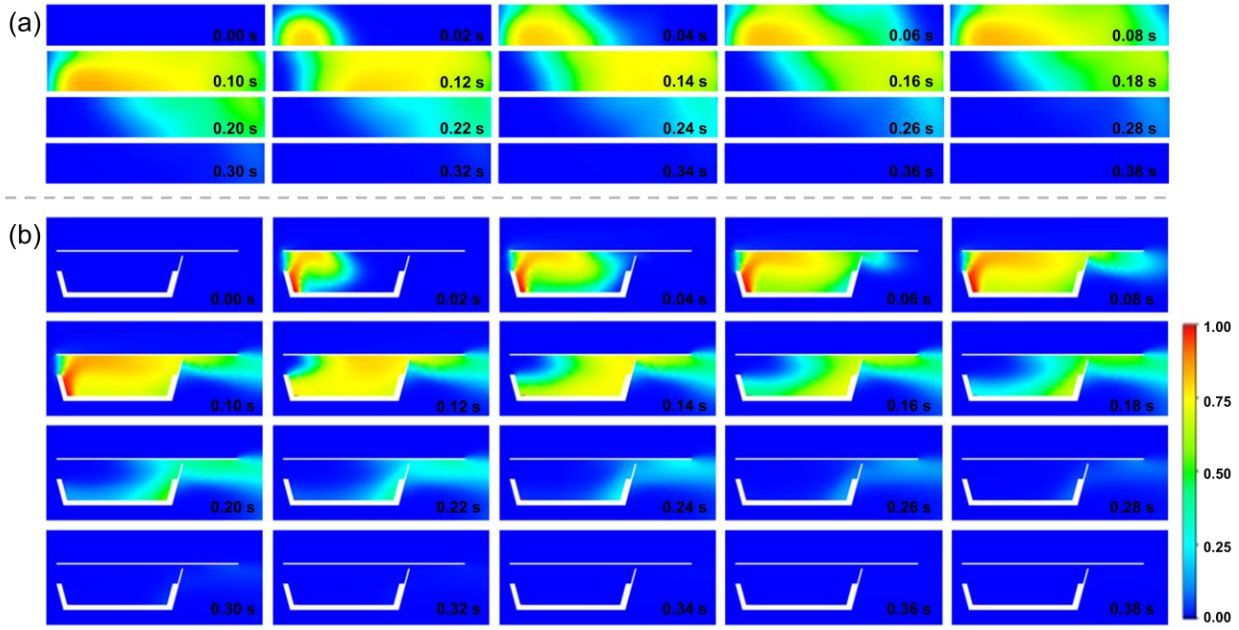

Figure S16. MoO_3 concentration evolution in the evolved APCVD growth process. (a) top view, (b) cross-sectional view.

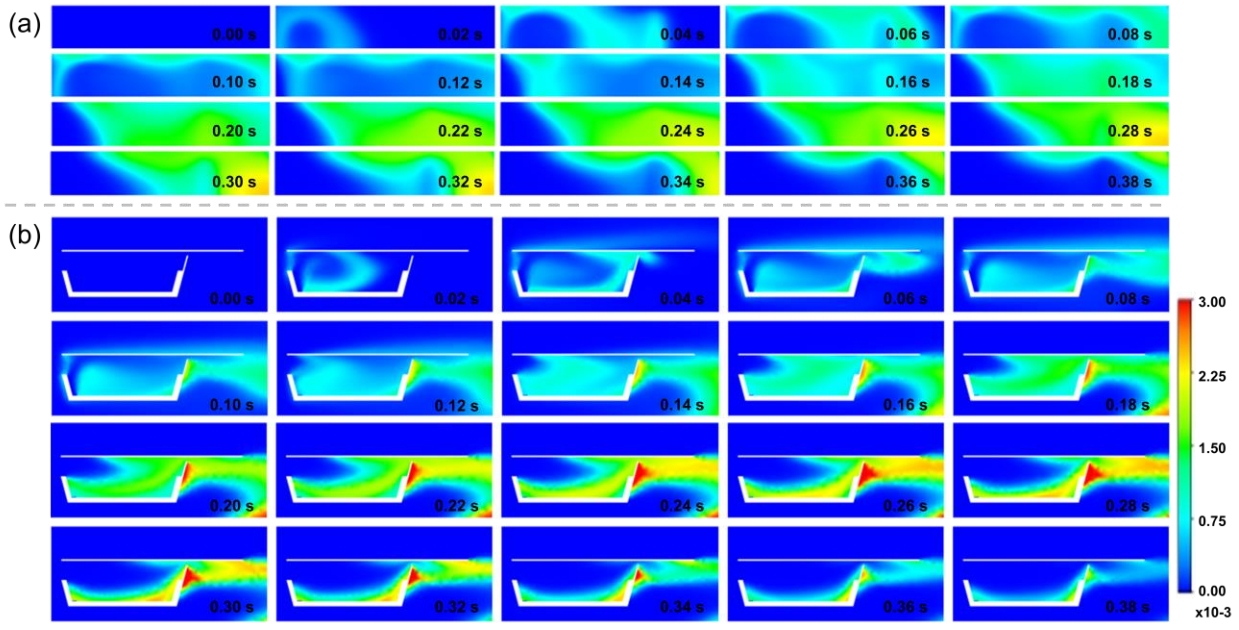

Figure S17. $MoSe_2$ concentration evolution in the evolved APCVD growth process. (a) top view, (b) cross-sectional view.

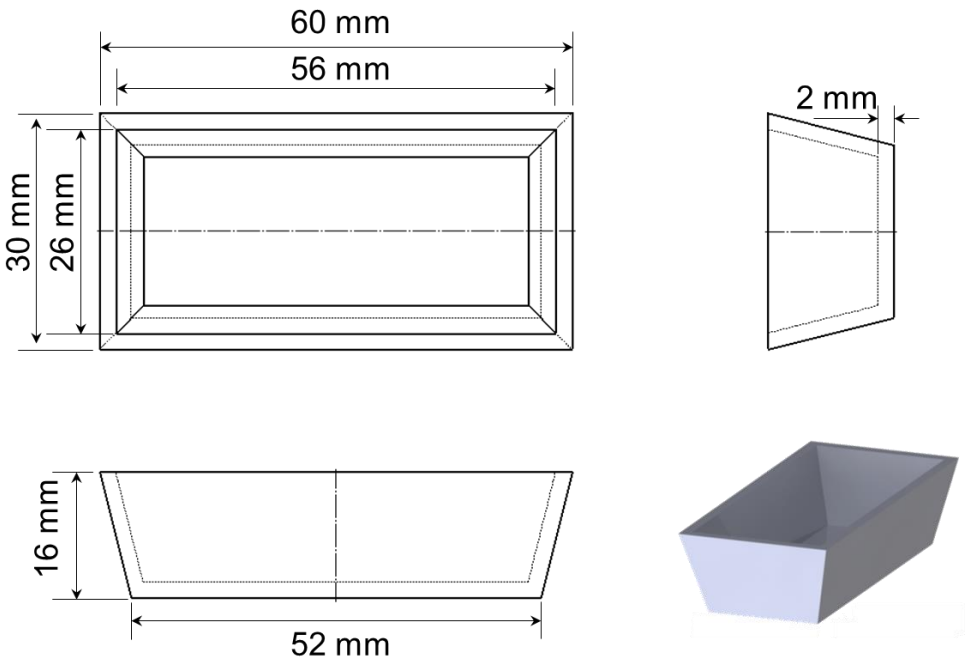

Figure S18. The structure and dimensions of the MoO_3 crucible.